overall size of the matrix lattice. This is independent of the size or number of precipitates, as well as of the severity of the field that surrounds them.

(iii) Scattering coherency from precipitates can influence the intensity from the matrix when the structures of the precipitate and matrix are similar enough to introduce overlapping amplitudes of scattering.

(iv) In the mixed–partitioned state only two matrix peaks may be apparent. One appears sharp and the second is broad. The sharp peak is a mixture of the Bragg and SD peaks, which tend to be located very near each other, while the broad peak is a quasiline. Consequently, matrix scattering may appear as a doublet.

(v) Precipitate scattering includes direct scattering from precipitates and voids as well as a cross term. The cross term may become negligible when no overlap occurs between the precipitate and void amplitude functions. In most cases, the shape of the precipitate scattering is primarily influenced by the size and shape of the precipitates. Displacement fields from other precipitates can interact and produce additional broadening. Partitioning in the case of precipitate scattering is not likely to be evident, although a peak shift and asymmetry resulting from strain may exist.

The author acknowledges his many discussions with Dr Satish Rao, dealing with the works of Krivoglaz and co-workers and the 1971 paper by Dederichs. These interactions on the diffraction effects of severely distorted lattices, as well as notes on these papers and computer simulations, were of considerable value in the author's development of the approach given in this paper. This work was made possible with the support of NSF Grant DMR-881 8013.

References

BARABASH, R. I. & KRIVOGLAZ, M. A. (1978). *Fiz. Met. Metalloved.* **45**, 7–18.

BARABASH, R. I. & KRIVOGLAZ, M. A. (1981). *Fiz. Met. Metalloved.* **51**, 903–916.

CULLITY, B. D. (1978). *Elements of X-ray Diffraction.* Reading, MA: Addison-Wesley.

DEDERICHS, P. H. (1970). *Phys. Rev. B*, **1**, 1306–1317.

DEDERICHS, P. H. (1971). *Phys. Rev. B*, **4**, 1041–1050.

DOBROMYSLOV, A. V. (1976). *Phys. Met. Metallogr.* **42**, 91.

DOBROMYSLOV, A. V. (1980). *Phys. Met. Metallogr.* **50**, 118.

GANZHUILA, N. N., KOZLOVA, L. YE. & KOKORIN, V. V. (1981). *Phys. Met. Metallogr.* **52**, 106–111.

HOLÝ, V. (1984). *Acta Cryst.* A**40**, 675–679.

IIDA, S., LARSON, B. C. & TISCHLER, J. Z. (1988). *J. Mater. Res.* **3**, 267–273.

KRIVOGLAZ, M. A. (1959). *Fiz. Met. Metalloved.* **7**, 650.

KRIVOGLAZ, M. A. (1960). *Fiz. Met. Metalloved.* **9**, 641.

KRIVOGLAZ, M. A. (1961). *Fiz. Met. Metalloved.* **10**, 169, 465.

KRIVOGLAZ, M. A. & HAO, T'YU (1969). *Fiz. Met. Metalloved.* **27**, 3–15.

LARSON, B. C., IIDA, S., TISCHLER, J. Z., LEWIS, J. D., ICE, G. E. & HABENSCHUSS, A. (1987). *Mater. Res. Soc. Symp. Proc.* **82**, 73–78.

LARSON, B. C. & SCHMATZ, W. (1974). *Phys. Rev. B*, **10**, 2307–2314.

MOSS, S., SPARKS, C. & ICE, G. (1992*a*). *Phys. Rev. B*, **45**, 2662–2676.

MOSS, S., SPARKS, C. & ICE, G. (1992*b*). *Phys. Rev. Lett.* **68**, 863–866.

SCHWARTZ, L. H. & COHEN, J. B. (1987). *Diffraction from Materials.* New York: Springer-Verlag.

TRINKHAUS, H. (1971). *Z. Angew. Phys.* **31**, 229.

WARREN, B. E. (1969). *X-ray Diffraction.* Reading, MA: Addison-Wesley.

Acta Cryst. (1993). A**49**, 781–789

Modelling Electrostatic Potential from Experimentally Determined Charge Densities. I. Spherical-Atom Approximation

BY NOUR-EDDINE GHERMANI, NOUZHA BOUHMAIDA AND CLAUDE LECOMTE*

Laboratoire de Minéralogie-Cristallographie et Physique Infrarouge–URA CNRS 809, *Université de Nancy* I, *Faculté des Sciences, BP* 239, 54506 *Vandoeuvre-lés-Nancy CEDEX, France*

(*Received* 25 *November* 1992; *accepted* 14 *May* 1993)

Abstract

Observations of the experimental electrostatic potential obtained from $X-X$ spherical electron density can be used to derive point charges centred on the atoms. This is applied to a pseudopeptide, *N*-acetyl-α,β-dehydrophenylalanine methylamide. The experimentally determined charges are consistent whatever the sampling points and 'follow' the atomic site when the conformation of the molecule

* To whom correspondence should be addressed.

changes. However, introduction of multipolar moments is necessary as soon as the aspherical part of the electron density is added.

Introduction

Molecular recognition is one of the key principles of computer methods for drug design. The interaction between drug and receptor is principally dependent on two factors. First, the drug must fit sterically into the active site of the receptor like a key in a lock. Second, for this lock–key interaction to be possible, site and drug must be electrostatically complementary.

When ligand A and B (receptor) are separated by more than *two van der Waals' radii*, they are at the molecular recognition stage and the electrostatic part E_{elect} of the interaction energy is predominant:

$$E_{elect} = \int V_B(\mathbf{r})\rho_A(\mathbf{r})\,d^3\mathbf{r}, \qquad (1)$$

where V_B is the electrostatic potential created by the receptor and ρ_A is the electronic density of the ligand A. This electrostatic energy must then be calculated with care and any change in $V_B(\mathbf{r})$ may modify the recognition process. Usually, the receptor is not well known and the drug molecule is often complex enough to prevent an *ab initio* calculation. The potential energy generally used in the molecular modelling is

$$V_{tot} = V_{conf} + \sum_{i<j}\sum [(Aij/r_{ij}^{12}) - (Bij/r_{ij}^{6})] + \sum_{i<j}\sum q_i q_i/\varepsilon r_{ij}, \qquad (2)$$

where V_{conf} is the conformational potential dependent on dihedral angles, torsion and stretching parameters, Aij and Bij (the Lennard-Jones parameters) are the repulsion and attraction coefficients, respectively, q_i is the atomic partial charge on atom i and ε is the effective dielectric constant. If all the mechanical and Lennard-Jones parameters are known from theory or experiment (Rasmussen, 1984), the partial charges remain inaccurate and depend strictly on the empirical calculations used and on other methods like those of Mulliken (1955), Bader (1990) or Hirshfeld (1977), which by partitioning determine the limits of each atom of the molecule and integrate the charge in this atomic volume.

In our studies of $X-X$ electron density in peptides and related compounds (Souhassou *et al.*, 1991, 1992; Lecomte, Ghermani, Pichon-Pesme & Souhassou, 1992; Pichon-Pesme, Lecomte, Wiest & Bénard, 1992) we now have a set of electron-density parameters calculated and refined for several different peptide molecules using (Hansen & Coppens, 1978)

$$\rho(\mathbf{r}) = \rho_c(r) + P_{val}\kappa'^3\rho_{val}(\kappa' r) + \sum_l \kappa''^3 R_{nl}(\kappa'' r)\sum_m P_{lm}Y_{lm}(\theta,\phi). \qquad (3)$$

κ' and κ'' are expansion–contraction coefficients and the third term of (3) accounts for the nonspherical deformation density. When no aspherical term is included in the density model, the refinement is known as 'κ refinement' (Coppens *et al.*, 1979) and is supposed to give the radial expansion and the charge of the atoms ($Q = Z - P_{val}$). Such a set of experimental charges was compared to theory for the DNA constituents (Pearlman & Kim, 1990). Furthermore, from the analytical expression for $\rho(r)$ [(3)], we are able to calculate the electrostatic potential at any point outside the molecule (Ghermani, Lecomte & Bouhmaida, 1993):

$$V(\mathbf{r}) = V_{core}(r) + V_{val}(r) + \Delta V(\mathbf{r}) \qquad (4)$$

with

$$V_{core}(r) = (Z/|\mathbf{r}-\mathbf{R}|) - \int_0^\infty [\rho_c(r')\,d^3r'/|\mathbf{r}-\mathbf{R}-\mathbf{r}'|]$$

$$V_{val}(r) = -\int_0^\infty [P_{val}\kappa'^3\rho_{val}(\kappa' r')\,d^3r'/|\mathbf{r}-\mathbf{R}-\mathbf{r}'|]$$

and

$$\Delta V(\mathbf{r}) = -4\pi\sum_{lm}[\kappa'' P_{lm}/(2l+1)]\Big[(1/\kappa''^{l+1}|\mathbf{r}-\mathbf{R}|^{l+1}) \times \int_0^{\kappa''|\mathbf{r}-\mathbf{R}|} t^{l+2}R_{nl}(t)\,dt + \kappa''^l|\mathbf{r}-\mathbf{R}|^l \times \int_{\kappa''|\mathbf{r}-\mathbf{R}|}^\infty (1/t^{l-1})R_{nl}(t)\,dt\Big]Y_{lm}(\theta',\phi').$$

Z is the charge of the nucleus, ρ_c and ρ_{val} are the core and valence electron densities of the free atom, respectively, and are calculated from the Clementi wave functions, θ' and ϕ' are the angular coordinates of the vector $(\mathbf{r}-\mathbf{R})$ (see Fig. 1). This potential will be referred to later as the experimental potential and can, in principle, be fitted by a set of point charges and multipole moments, if necessary, at the nuclear positions. As we have shown, the P_{lm} electron-density parameters [(3)] are transferable from a group of atoms in a molecule to the same group in another molecule (Pichon-Pesme, Lecomte & Lachekar, 1993), which means that our potential-fitted charges may be transferable and useful in

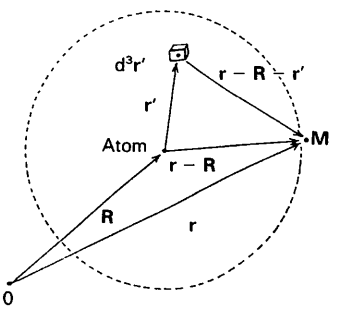

Fig. 1. Calculation of the electrostatic potential.

molecular-recognition processes or molecular modelling if we check that they are not conformation dependent.

This paper is divided into three parts. The first part describes the method used to obtain the potential-fitted charges. In the second part, the method is applied to the potential derived from the spherical part of the electron density ($P_{lm} = 0$) of the *N*-acetyl-α,β-dehydrophenylalanine methylamide molecule (hereafter referred to as AcΔ) (Souhassou *et al.*, 1992) (Fig. 2). The last part of the paper is devoted to the effect of the conformation of the molecule on the potential-fitted charges. The second paper of the series will discuss charges and multipole moments fitted to an electrostatic potential calculated from a multipolar refinement.

Calculation of the potential-derived charges

Use of the Householder triangularization method

The electrostatic potential of a given molecule can be calculated at any point outside the molecule from (4) as soon as a set of electron density parameters has been obtained for each atom of the molecule.

Let $V_{obs}(x,y,z)$ be the experimental potential of M given points (x_i,y_i,z_i) carefully sampled in the space. The problem is to get a set of N charges q_j centred on the atoms and satisfying the minimum of the function

$$\Delta = \sum_k^M |V_{obs}(k) - \sum_i (q_i/R_{ik})|^2.$$

This fit is possible, as shown in Fig. 3, which displays the electrostatic potentials of a positive and a negative oxygen atom calculated from Clementi wave functions. It can be noted that, at a distance greater than 2 Å, the potential curves may be very well fitted by a hyperbola $\pm q/R$. The situation is slightly more complicated for nonspherical atoms, where addition of multipole moments is necessary.

The solution is generally given by the conventional least-squares method, where the resolution is carried out algebraically using the normal matrix $A = [\partial^2\Delta/\partial q_i \partial q_j]$. The problem here is linear with respect to q_i; A becomes $A = [\sum_k^M 1/R_{ik}R_{jk}$, where $R_{ik}(R_{jk})$ is the distance from the observation point k to atom i (j). The matrix A is of dimension N and must be inverted. The determinant of A falls off very quickly with the increase in the number of atoms because it is a product of $1/R_{ik}$ terms. In the Householder triangularization method (Lascaux & Theodor, 1986), we solve the system of M linear equations $[B]$ $[q_i] = [V_{obs}]$, where B is an $M \times N$ matrix; B is not inverted but is transformed to a N-dimensional triangular matrix. This method is more flexible and the results are more stable, whatever the values of M and N. It has been implemented as a subroutine in the potential-calculation program *ELECTROS*, which is available from the authors (Ghermani, Bouhmaida & Lecomte, 1992). In none of the calculations has an electroneutrality constraint been applied.

The observation sampling

As shown earlier, the observed electrostatic potential can be calculated at any point of the space around a given molecule because it is calculated

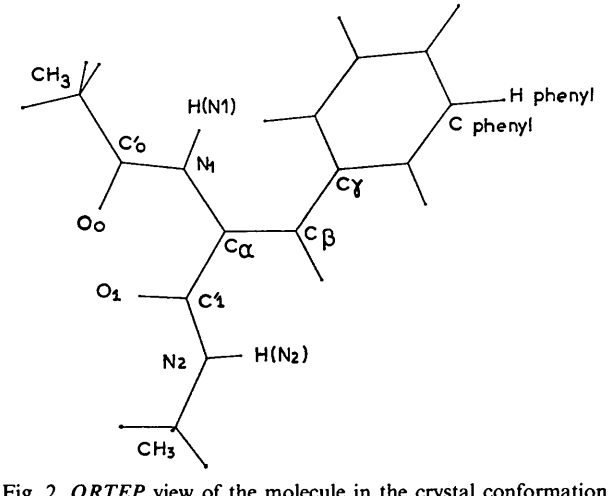

Fig. 2. *ORTEP* view of the molecule in the crystal conformation ($\varphi_0 = -56.81$, $\psi_0 = 148.71$, $\chi^2_0 = -39.13°$).

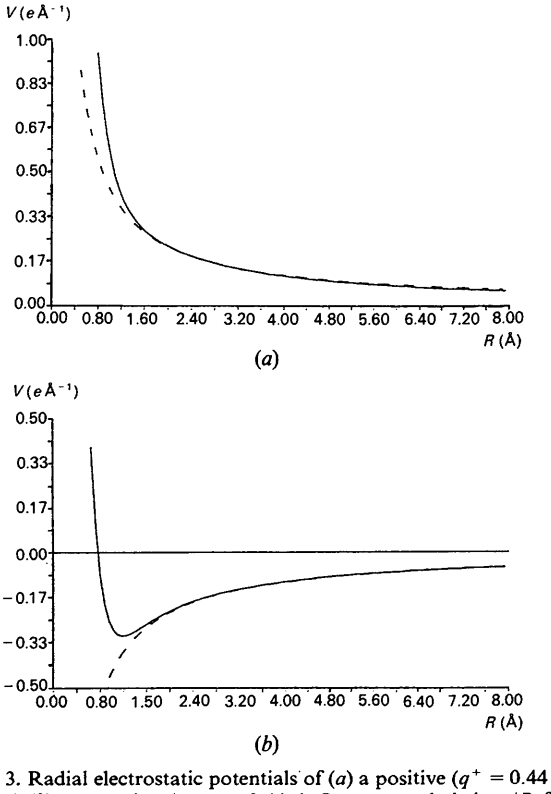

Fig. 3. Radial electrostatic potentials of (*a*) a positive ($q^+ = 0.44$ e) and (*b*) a negative ($q^- = -0.44$ e) O atom and their q/R fits (dashed lines).

analytically from the density parameters. In fact, the electrostatic interaction for molecular recognition occurs outside the molecule; the observation must be made on the van der Waals surface and further out of the molecule. For the observation points, spherical contours were built around each atom instead of a cubic grid; this has the advantage of taking into account the conformation and then the eventual folding of the molecule (see Fig. 4). The spherical grid also conforms better to the $\pm q/R$ function. We also used one or several shells around each atom from 2 to 8 Å. Furthermore, the observation points on one given sphere are equidistant: their coordinates θ and φ with respect to the same orthogonal axis centred at each atom are related by

$$\Delta\varphi = \ln\{\tan[(\theta + \Delta\theta)/2]\tan(\theta/2)\},$$

where $\Delta\theta = 15$ or 30° in our calculations; we found smaller steps unnecessary to fit the spherical potential. An observation point k was rejected if it was at a distance R_{ik} smaller than the radius of the first shell.

After the fit, a residual factor $R(V)$ is calculated as

$$R(V) = \Big[\sum_{k=1}^{M} |V_{\mathrm{obs}_k} - V_{\mathrm{calc}_k}|^2 \Big/ \sum_{k=1}^{M} V^2_{\mathrm{obs}_k}\Big]^{1/2}.$$

Application to *N*-acetyl-α,β-dehydrophenylalanine methylamide, AcΔ

Nondependence of the charges from the sampling points for the crystal-fixed conformation when $V(\mathbf{r})$ is calculated from a spherical refinement

The method was applied to *N*-acetyl-α,β-dehydrophenylalanine methylamide (Fig. 2). This is a pseudopeptide molecule with one double bond between C^α and C^β. Therefore, as shown by Souhassou *et al.* (1992), the two peptide bonds are nonequivalent and we do not expect the same charges on the C, N and O atoms of the two peptide links. Table 1 gives the net charges averaged on chemically equivalent atoms obtained from different samplings of points. These values can be compared with the net charges q obtained after the spherical refinement ($q = Z - P_{\mathrm{val}}$) and used to generate the electrostatic potential. Each line of Table 1 gives the minimum radius R_{min}, the $\Delta\theta$ increment, the calculated charges, the number of observations, the residual R factor and the total charge of the molecule. The last two lines correspond to a calculation that includes 7 and 13 shells ($R_{\mathrm{min}} = 2$ Å) from 2 to 8 Å in steps of 1 and of 0.5 Å, respectively. The fit is excellent whatever the sampling used, as shown by the R values, which range from almost 0 to 1% for 12000 points.

The values obtained for the different types of atoms are consistent; in more detail, the charges obtained from a minimum radius of 2 Å are different by several per cent: this is because $V(r)$ varies faster than q/R at short distances (Fig. 3).

To take into account the steric interactions and the nature of the atoms, another calculation was performed with a minimum radius equal to a multiple of the van der Waals radii of each atom ($r_C = 1.7$, $r_O = 1.52$, $r_N = 1.55$, $r_H = 1.2$ Å); all the results are given in the supplementary material.* The charges obtained are, as expected, equal to those of Table 1, to within less than 10^{-2} e, and the R factors are less than 10^{-3}. To show the excellence of this fit, Fig. 5 compares the observed electrostatic potential on a peptide plane (*a*) with the potential calculated from

$$V_i(r) = \sum_{j=1}^{N} q_j |r_{ij}|^{-1} \qquad (5)$$

(Fig. 5*b*), where the q_j are the fitted charges against the potential at a sample of points chosen at two van der Waals radii. Fig. 5(*c*) gives the difference between the two maps. As soon as we look at a distance of more than 2 Å, the two calculations lead to almost exactly the same potential. On the other hand, the fitted charges from the experimental potential are not very different from the charges obtained from the P_{val} parameters. This is the expected result of a spherical refinement according to the Gauss theorem because almost all of the charge on the atoms is inside the volume in which the sampling points are chosen. As shown in Fig. 5(*d*), the potential calculated from point charges equal to $q = (Z - P_{\mathrm{val}})$ differs significantly from the observed one (Fig. 5*a*).

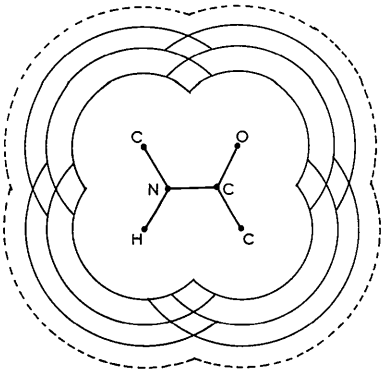

Fig. 4. Sampling-point shells for a peptide link.

* Tables of fitted charges derived from sampling points based on van der Waals' radii for AcΔ in the crystal conformation, experimental and fitted electrostatic potentials of a peptide link in conformation III and experimental and fitted potentials in the plane perpendicular to the phenyl ring of AcΔ in conformation IV (contours -0.01 e Å^{-1}) have been deposited with the British Library Document Supply Centre as Supplementary Publication No. SUP 71132 (7 pp.). Copies may be obtained through The Technical Editor, International Union of Crystallography, 5 Abbey Square, Chester CH1 2HU, England.

Table 1. *Non-dependence of the charges on the sampling points for AcΔ in the crystal conformation*

		C'_0	O_0	C'_1	O_1	N_1	$H(N_1)$	N_2	$H(N_2)$	C^α	C_{phenyl}	H_{phenyl}	CH_3			
Net charge*		0.132	−0.370	−0.097	−0.440	−0.306	+0.246	−0.083	0.237	−0.098	−0.101	+0.156	0.113			
	κ	1.020	0.974	0.999	0.977	0.989	1.093	1.001	1.090	1.001	0.997	1.154				
R_{min} (Å)	$\Delta\theta$ (°)													N_{obs}	R (%)	Σq_i
2	30	0.184	−0.439	−0.080	−0.499	−0.335	0.221	−0.099	0.224	−0.060	−0.080	0.134	0.083	275	0.008	−0.180
4	30	0.171	−0.422	−0.099	−0.487	−0.327	0.246	−0.079	0.235	−0.093	−0.106	0.156	0.064	128	0.000	−0.189
6	30	0.171	−0.422	−0.099	−0.486	−0.326	0.246	−0.079	0.237	−0.095	−0.106	0.156	0.063	94	0.000	−0.189
6	15	0.171	−0.422	−0.099	−0.487	−0.327	0.246	−0.079	0.237	−0.094	−0.107	0.156	0.064	432	0.000	−0.189
8	15	0.171	−0.422	−0.098	−0.487	−0.326	0.246	−0.079	0.237	−0.096	−0.106	0.156	0.065	361	0.000	−0.189
2–8	30	0.187	−0.439	−0.096	−0.499	−0.311	0.215	−0.077	−0.222	−0.054	−0.097	0.143	0.074	5755	0.011†	−0.188
2–8	30	0.189	−0.438	−0.108	−0.495	−0.315	0.218	−0.070	0.221	−0.049	−0.095	0.144	0.072	11966	0.0109	−0.188

* Starting values to generate the electrostatic potential.
† R calculated on 11966 points.

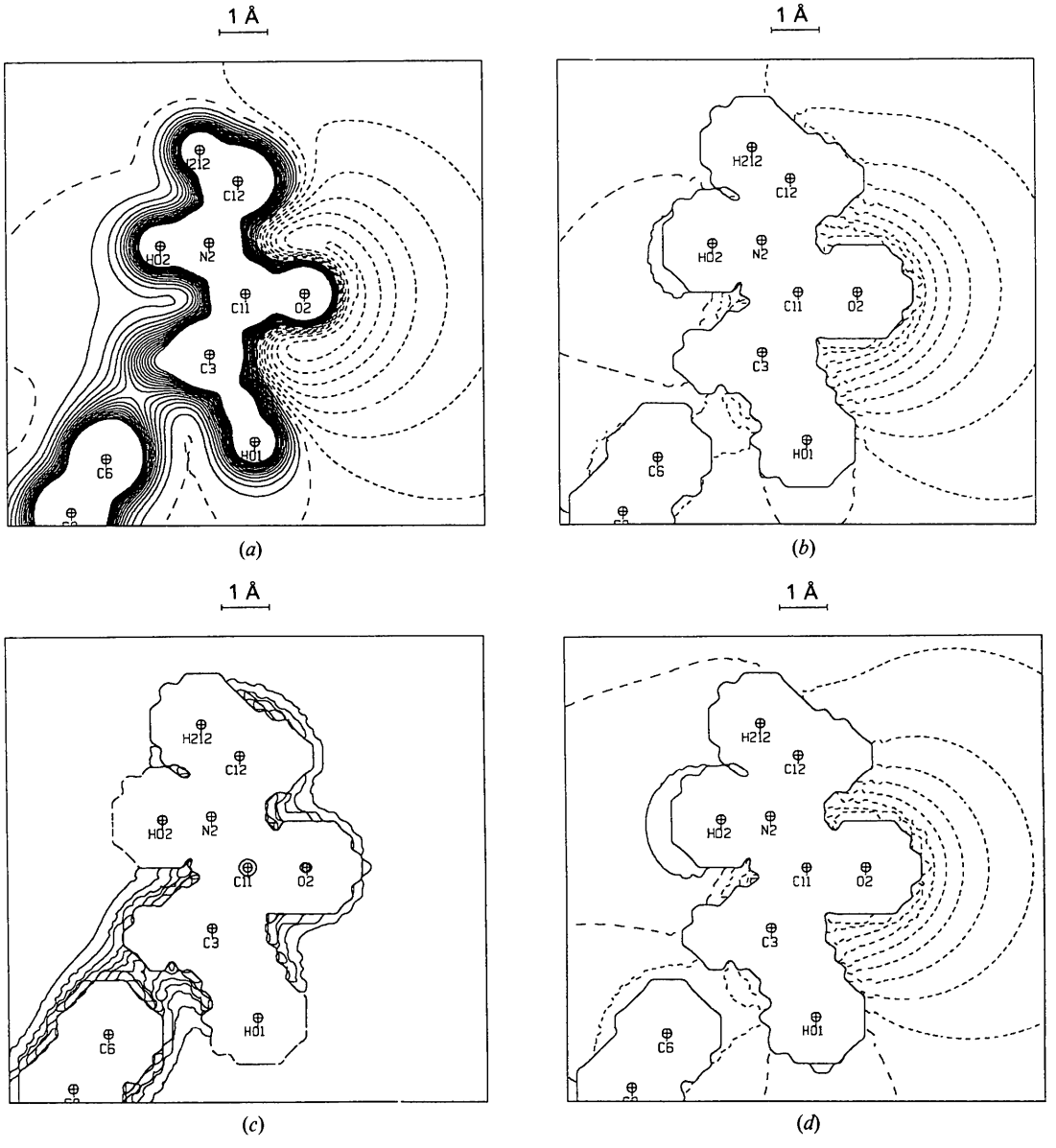

Fig. 5. Electrostatic potential maps of a peptide link of AcΔ: (*a*) observed potential V_{obs} from (4); (*b*) calculated potential V_{cal} from (5); (*c*) $V_{obs} - V_{cal}$; (*d*) potential calculated with (5) and $q = Z - P_{val}$. Contours are 0.05 e Å^{-1} (1 e Å^{-1} = 332.1 kcal mol^{-1}). Zero and negative contours are dashed.

As pointed out before, no electroneutrality constraint was used in the calculations. The sum of the fitted charges over the molecule is about -0.19 e against -0.02 e for the experimental net charges. If we distribute the -0.19 e to all the atoms of the molecule taking into account the electronic weight of each of them, we get new charges that are statistically equal, within 10^{-2} e, to the previous ones. It confirms that a neutrality constraint is not necessary because the error on the model electron density is 0.05 e Å^{-3} (Souhassou *et al.*, 1992).

Fitted charges for other conformations of the molecule from spherical refinement

This set of charges was calculated for the crystal conformation. It is necessary to check that the set obtained is stable when the molecular conformation changes. As the electron density of the molecule does not change significantly with conformation (Pichon-Pesme, Lecomte & Lachekar, 1993), we kept the P_{val} and κ values to calculate new potentials for several molecule conformations, changing the $\varphi(C^{\alpha}$–N), $\psi(C^{\alpha}$–C′), $\chi^2(C^{\beta} - C^{\gamma})$ and $\varphi + \psi$ torsion angles. We checked that each of these chosen conformations was sterically possible (El-Masdouri, 1989). The four *ORTEP* views are given in Fig. 6 with their associated φ, ψ and χ^2 angles. The calculated potential does not change in the close vicinity of the atoms but the contour curves are different in the intermolecular region, as shown, for example, in Figs. 7(*a*) and (*b*), which represent the electrostatic potential on the same peptide plane as that of Fig. 5 ($N_2C_{11}O_2$) for conformations I and II and their fitted potential (Figs. 5*c* and *d*). The fit of the q_i to the observed potential is excellent (Table 2). Furthermore, the

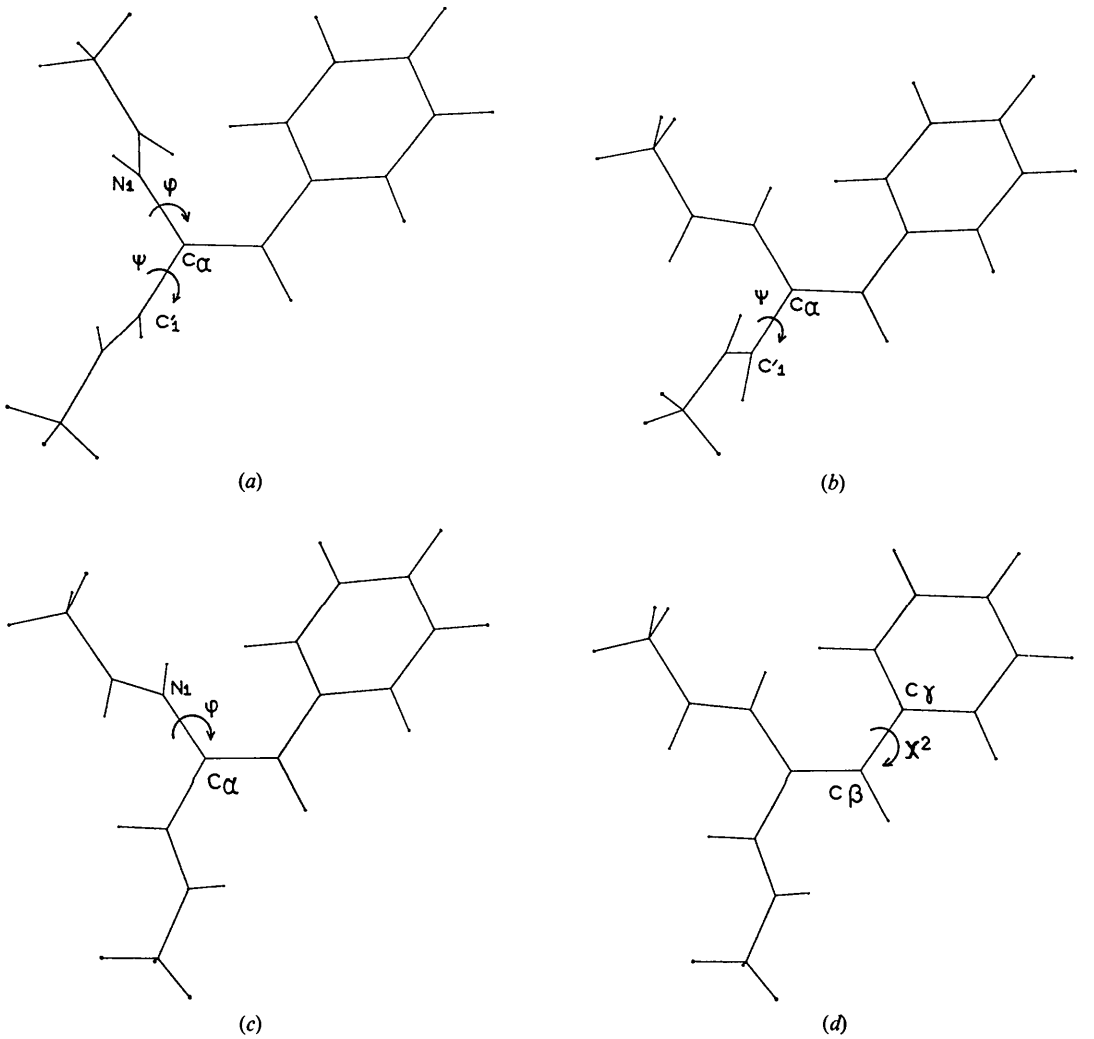

Fig. 6. *ORTEP* views of the chosen conformations: (*a*) conformation I, $\varphi = -88.8$, $\psi = 89.30$, $\chi^2 = -39.13°$; (*b*) conformation II, $\varphi = -56.81$, $\psi = 120.71$, $\chi^2 = -39.13°$; (*c*) conformation III, $\varphi = -76.81$, $\psi = 148.71$, $\chi^2 = -39.13°$; (*d*) conformation IV, $\varphi = -56.81$, $\psi = 148.71$, $\chi^2 = -22.13°$.

Table 2. *Nondependence of the charges on the molecular conformation*

R_{max} (Å)	$\Delta\theta$ (°)	C'_0	O_0	C'_1	O_1	N_1	$H(N_1)$	N_2	$H(N_2)$	C^α	C_{phenyl}	H_{phenyl}	CH_3	N_{obs}	R (%)	Σq_j
Conformation I																
3.5	30	0.175	−0.423	−0.102	−0.487	−0.332	0.247	−0.075	0.235	−0.082	−0.109	0.157	0.063	337	0.0005	−0.189
8.5	30	0.174	−0.423	−0.101	−0.487	−0.331	0.247	−0.077	0.236	−0.085	−0.108	0.156	0.064	4684	0.0003	−0.189
Conformation II																
3.5	30	0.176	−0.424	−0.103	−0.486	−0.330	0.246	−0.077	0.237	−0.085	−0.107	0.155	0.063	353	0.0008	−0.189
8.5	30	0.174	−0.423	−0.101	−0.486	−0.326	0.245	−0.077	0.237	−0.091	−0.107	0.156	0.067	4765	0.0005	−0.189
Conformation III																
3.5	30	0.176	−0.424	−0.100	−0.487	−0.328	0.246	−0.077	0.237	−0.091	−0.107	0.155	0.062	340	0.0006	−0.189
8.5	30	0.173	−0.423	−0.099	−0.487	−0.324	0.245	−0.077	0.237	−0.094	−0.106	0.156	0.063	4750	0.0004	−0.189
Conformation IV																
3.5	30	0.177	−0.424	−0.099	−0.488	−0.330	0.247	−0.077	0.237	−0.090	−0.106	0.155	0.062	328	0.0006	−0.189
8.5	30	0.175	−0.424	−0.098	−0.487	−0.328	0.246	−0.078	0.237	−0.094	−0.107	0.156	0.063	4749	0.0004	−0.189

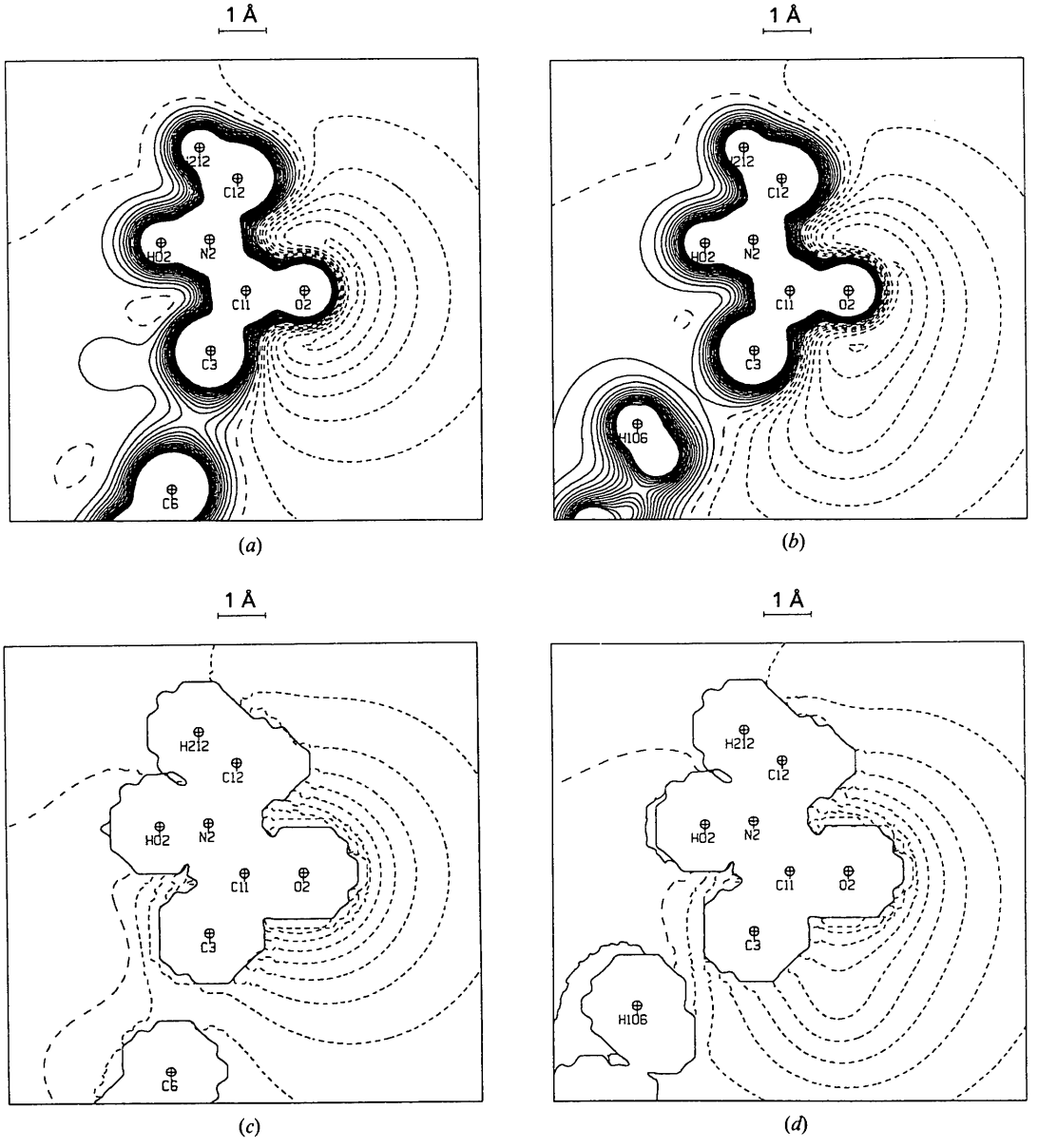

Fig. 7. Electrostatic potential maps of a peptide link of AcΔ for conformations I and II: (*a*) and (*b*) observed potential; (*c*) and (*d*) fitted potential. Same contours as in Fig.5.

fitted charges are close to those obtained for the crystal-fixed conformation; the differences do not exceed 0.05 e. The fitted charges are then independent of the molecular conformation when the spherical refinement parameters are used to calculate the observed potential.

Concluding remarks

It is possible to obtain reliable point charges on atoms by fitting the electrostatic potential of the molecule when this property is calculated from the spherical part of the electron density or from a κ refinement. The partial charges found are consistent and are independent of both the choice of the sample points, when their minimum distance from the atom is greater than 2 Å, and the molecular conformation. This makes possible the transferability of these important quantities to other molecules.

The next problem is the assignment of charges when the potential calculation includes the aspherical part. As a first test of the method, we took the multipole parameters of the water molecule in the crystal of Leu-enkephalin.$3H_2O$ (Pichon-Pesme, Lecomte, Wiest & Bénard, 1992). Fig. 8(*a*) gives the electrostatic potential including the dipole and quadrupole components of the electron density [see (3) and (4)]. First, this experimental electrostatic potential was fitted by point charges on a single shell corresponding to two van der Waals radii. The fit was not very good ($R = 19\%$) and led to $q_O = -0.89$ and $q_H = 0.44$ e. To improve the quality of the fit, atomic multipole moments were included up to the dipole level for H atoms and to the quadrupole level for O atoms. The R factor fell to 0.0017 and the charges obtained were $q_O = -0.54$ and $q_H = 0.27$ e; the potential map (Fig. 8*b*) is almost identical to the experimental one. The introduction of these multipolar moments is then necessary to improve the point-charges fitting method. This is in very good agreement with the results of Stone & Price (1988), who showed that the atomic distributed multipoles are needed to calculate the molecular energy. Further work is in progress to apply this correction to peptide molecules.

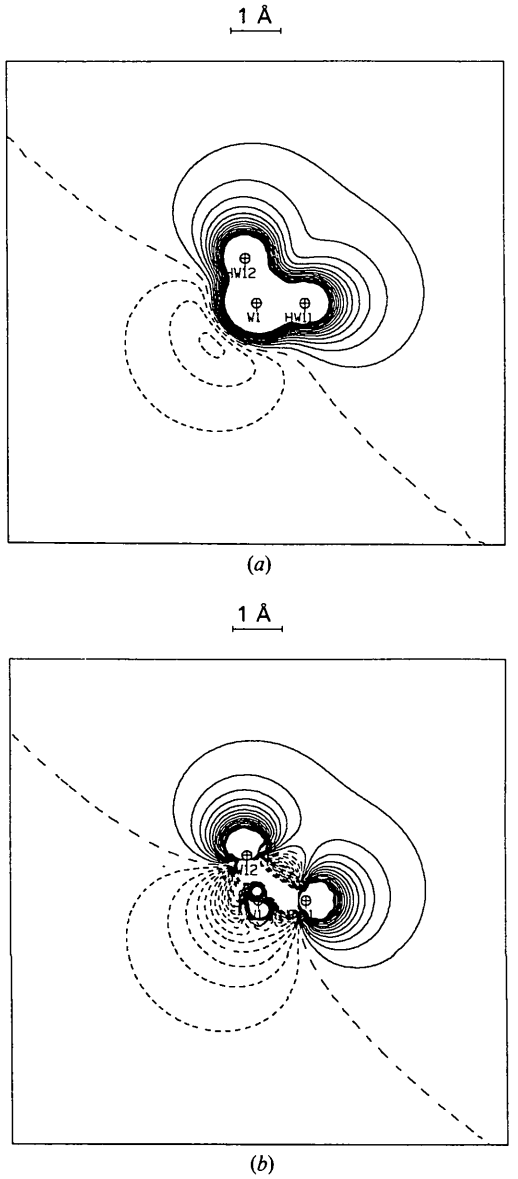

Fig. 8. Electrostatic potential maps of a water-molecule solvate in Leu-enkephalin calculated from a multipole electron-density model and fitted by (*a*) the point-charges model and (*b*) the point charges and dipole and quadrupole moments.

We would like to thank Mr Moussa Mamoudou and Professor A. Henrot of the Department of Mathematics of the University of Nancy I for fruitful discussions. The financial support of the CNRS and of the University of Nancy I is gratefully acknowledged.

References

BADER, R. F. W. (1990). *Atoms in Molecules – a Quantum Theory*. Oxford Univ. Press.

COPPENS, P., GURU ROW, T. N., LEUNG, P., STEVENS, E. D., BECKER, P. J. & YANG, Y. W. (1979). *Acta Cryst.* A**35**, 63–72.

EL-MASDOURI, L. (1989). Thèse, pp. 48–49, Univ. de Nancy I, France.

GHERMANI, N., BOUHMAIDA, N. & LECOMTE, C. (1992). *ELECTROS: Computer Program to Calculate Electrostatic Properties from High Resolution X-ray Diffraction*. Internal report URA CNRS 809. Univ. de Nancy I, France.

GHERMANI, N., LECOMTE, C. & BOUHMAIDA, N. (1993). *Z. Naturforsch. Teil A*, **48**, 91–98.

HANSEN, N. & COPPENS, P. (1978). *Acta Cryst.* A**34**, 909–921.

HIRSHFELD, F. L. (1977). *Theor. Chim. Acta*, **44**, 129–138.

LASCAUX, P. & THEODOR, R. (1986). *Analyse Numérique Matricielle Appliquée à l'Art de l'Ingénieur*, Vol. I. Paris: Masson.

LECOMTE, C., GHERMANI, N., PICHON-PESME, V. & SOUHASSOU, M. (1992). *J. Mol. Struct. (Theochem)*, **255**, 241–260.

MULLIKEN, R. S. (1955). *J. Chem. Phys.* **23**, 1833–1841.

PEARLMAN, D. A. & KIM, S.-H. (1990). *J. Mol. Biol.* 171–187.

PICHON-PESME, V., LECOMTE, C. & LACHEKAR, H. (1993). In preparation.
PICHON-PESME, V., LECOMTE, C., WIEST, R. & BÉNARD, M. (1992). *J. Am. Chem. Soc.* **114**, 2713–2715.
RASMUSSEN, K. (1984). In *Potential Energy Functions in Conformational Analysis. Lecture Notes in Chemistry*, Vol. 37. New York: Springer-Verlag.
SOUHASSOU, M., LECOMTE, C., BLESSING, R. H., AUBRY, A., ROHMER, M. M., WIEST, R., BÉNARD, M. & MARRAUD, M. (1991). *Acta Cryst.* B**47**, 253–266.
SOUHASSOU, M., LECOMTE, C., GHERMANI, N., ROHMER, M. M., WIEST, R., BÉNARD, M. & BLESSING, R. H. (1992). *J. Am. Chem. Soc.* **114**, 2371–2382.
STONE, A. J. & PRICE, S. L. (1988). *J. Phys. Chem.* **92**, 3325–3335.

SHORT COMMUNICATIONS

Contributions intended for publication under this heading should be expressly so marked; they should not exceed about 1000 *words; they should be forwarded in the usual way to the appropriate Co-editor; they will be published as speedily as possible.*

Acta Cryst. (1993). A**49**, 789–790

Comment on *Correlating the optical rotation of α-quartz with a skew matrix of a dielectric tensor* by Szu-Lin Chen (1993).

By A. M. GLAZER, *Department of Physics, Clarendon Laboratory, Parks Road, Oxford OX1 3PU, England*

(*Received* 2 *April* 1993; *accepted* 25 *May* 1993)

Abstract

A theory of optical rotation in α-quartz that was recently published by Chen [*Acta Cryst.* (1993), A**49**, 148–154] results in optically inactive directions perpendicular to the optic axis. It is pointed out here that this conclusion is not in accordance with either symmetry considerations or the observed experimental evidence.

Recently, Chen (1993) described a theoretical treatment of the optical rotation in α-quartz. The procedure involved calculations of the polarizabilities of individual SiO_4 tetrahedra within a unit cell and resulted in the conclusion that, in addition to optically inactive directions 33.83° from the optic axis, there should also be inactive directions *along the diad axes of quartz*. My purpose in writing this note is to point out that this cannot be correct and indicate some of the errors made in the theory used.

Now, it is well known that there are inactive directions at a particular azimuthal angle to the optic axis. The effect is caused by the fact that the rotation *perpendicular* to the optic axis is of opposite sign to that *along* the optic axis. Chen quotes Wahlstrom (1979) as giving this angle as 33.83° to the optic axis, but in fact this is a misunderstanding of what Wahlstrom meant by the phrase 'plate inclined at 56.17° to the optic axis' [this angle was actually determined, for example, by Szivessy & Münster (1934); it was also quoted in the well known book of Nye (1987)].

Moreover, the idea that there are additional inactive directions along the diad axes of quartz would appear to violate crystal symmetry, since the form of the gyration tensor for a trigonal crystal like quartz would require the gyration to be the same for *all* directions perpendicular to the optic axis, including the diad axes. All measurements made perpendicular to the optic axis [for example, those of Szivessy & Münster (1934), Bruhat & Grivet (1935), Konstantinova, Ivanov & Grechushnikov (1969), Kobayashi & Uesu (1983), Kobayashi, Uesu & Takehara (1983), Horinaka, Tomii, Sonomura & Miyauchi (1985), Moxon & Renshaw (1990) and Moxon, Renshaw & Tebbutt (1991)] agree in indicating that the optical rotation perpendicular to the optic axis has a measurable value opposite in sign to that along the optic axis, so it cannot be zero for *any* direction perpendicular to the optic axis.

In addition, Chen quotes a 'prediction' of Wahlstrom (1979) that 'light travelling at right angles to the optic axis is rotated but in opposite sense to that propagated along the optic axis'. It is fair to point out that this is a misunderstanding of language, in that Wahlstrom makes no such prediction but correctly reports this as a fact, presumably on the basis of his knowledge of the well known experimental evidence already published. Wahlstrom's book, excellent though it is, is a student textbook on optical crystallography in general and is not, therefore, a primary reference for work on optical rotation. There is, in fact, a vast amount of literature, going back to the last century, in which the many theories of optical rotation in crystals are described [for a general discussion, see, for instance, Glazer & Stadnicka (1986) and Devarajan & Glazer (1986)].

So what, then, is wrong with Chen's calculation? I believe that the answer to this question lies in the oversimplification of the theory used. For instance, the calculation is made by combining together the polarizability effects of a few tetrahedra within a unit cell. This treatment, however, ignores the fact that the tetrahedra exist within a *crystal*, *i.e.* an infinitely extending structure. By restricting the calculation to a few tetrahedra within a unit cell, the author ignores the combined contributions of all the other atoms in the crystal. In any proper treatment of optical rotation in crystals, it is necessary to sum the effective electric fields throughout the whole crystal, for example *via*